

CONF-76-0831-3

76-126

Note: This is a draft of a paper being submitted for publication. Contents of this paper should not be quoted nor referred to without permission of the authors.

## ELECTRONIC STRUCTURE OF THE F CENTER IN THE ALKALINE EARTH OXIDES

T. M. Wilson and R. F. Wood

NOTICE

This report was prepared as an account of work sponsored by the United States Government. Neither the United States nor the United States Energy Research and Development Administration, nor any of their employees, nor any of their contractors, subcontractors, or their employees, makes any warranty, express or implied, or assumes any legal liability or responsibility for the accuracy, completeness or usefulness of any information, apparatus, product or process disclosed, or represents that its use would not infringe privately owned rights.

By acceptance of this article, the publisher or recipient acknowledges the U.S. Government's right to retain a nonexclusive, royalty-free license in and to any copyright covering the article.

SOLID STATE DIVISION  
OAK RIDGE NATIONAL LABORATORY  
Operated by  
UNION CARBIDE CORPORATION  
for the  
ENERGY RESEARCH AND DEVELOPMENT ADMINISTRATION  
Oak Ridge, Tennessee

MASTER

August 1976

CONTRACT NO. W-7405-ENG-26

## ELECTRONIC STRUCTURE OF THE F CENTER IN THE ALKALINE EARTH OXIDES\*

T. M. Wilson

Department of Physics, Oklahoma State University  
Stillwater, Oklahoma 74074

and

R. F. Wood

Solid State Division, Oak Ridge National Laboratory  
Oak Ridge, Tennessee 37830

## ABSTRACT

The energy levels and wave functions of the ground and first few singlet and triplet excited states of the F center in MgO, CaO and SrO have been calculated as a function of the nearest neighbor ion positions. Configuration coordinate curves for  $A_{1g}$ ,  $E_g$  and  $T_{2g}$  displacements have been constructed and used to interpret the absorption and luminescence bands of the F center. The energy of the  $^1A_{1g} \rightarrow ^1T_{1u}$  transition was set near the experimental value in each case by adjusting certain parameters in the model. The calculated energy level schemes partially support the interpretations of published experimental data on the luminescence bands in MgO and CaO and suggest that the  $^3T_{1u} \rightarrow ^1A_{1g}$  luminescence in SrO should occur at roughly 0.4 eV. A luminescence band associated with the F center in SrO has not yet been reported. Our calculations of the Jahn-Teller coupling constants indicate that the  $^3T_{1u}$  state is strongly coupled to the  $E_g$  vibrational mode in CaO and to the  $T_{2g}$  mode in MgO and SrO.

---

\*Research sponsored by the U. S. Energy Research and Development Administration under contract with Union Carbide Corporation.

## I. INTRODUCTION

In this paper we shall describe results of calculations that we have made on the F center in MgO, CaO and SrO; some of these have already been reported but many have not. The F center in an alkaline-earth oxide is an  $O^{2-}$  vacancy at which two electrons are trapped. It and its one-electron counterpart, the  $F^+$  center, are among several defect centers in the alkaline-earth oxides that have received considerable attention from experimentalists in recent years.<sup>1</sup> These studies have added greatly to our knowledge of the optical and paramagnetic properties of defects in these materials. The experimental situation is to be contrasted with the theoretical one in which a scarcity of reliable calculations of the electronic states of these centers and their behavior with lattice distortions has impeded the fundamental understanding of the experimental results. These calculations are more difficult in the alkaline-earth oxides than in the alkali halides due in part to the greater polarizability of the  $O^{2-}$  ion as compared to a halide ion. The polarizability of the  $O^{2-}$  ion is difficult to treat adequately because of its strong dependence on its crystalline environment, e.g., the charge at the defect site. Also it should be kept in mind that the  $O^{2-}$  ion is not stable in free space; only through the action of the Madelung potential is it stabilized in the crystal.

The model used to make the calculations reported in this paper will be more fully described elsewhere. It is based on methods previously developed for point defects in alkali-halides, e.g., the F center,<sup>2-4</sup> U center,<sup>5,6</sup> M center<sup>7</sup> and excitons.<sup>8</sup> This model emphasizes the importance of the electronic structure of the ions neighboring the defect, the

electronic and ionic polarization of the lattice, and lattice distortion and its effects on the energy levels of the defect. The structure on the neighboring ions gives rise to coulomb, exchange and overlap repulsive contributions to the energy. Although these contributions may often be small relative to the Madelung energy, they change significantly from state to state and must be included. The electronic and ionic polarization effects are also important for the energy and are frequently crucial for the determination of the wave functions. Through these polarization effects, rather small changes in energy may be accompanied by large changes in the spatial extent of the wave functions. The inclusion of lattice distortion or relaxation is essential for determining the Stokes shift between absorption and emission, and for calculating the electron-phonon coupling at the defect site. Our computer programs enable us to calculate this coupling for  $A_{1g}$ ,  $E_g$  and  $T_{2g}$  modes of lattice distortion. This is particularly important for centers whose optical bands show vibronic structure such as the emission spectrum from the triplet state of the F center in CaO.

### III. REVIEW OF PREVIOUS WORK

F center absorption bands have been identified in the spectra of MgO, CaO, SrO and BaO, but the corresponding emission spectra have been positively identified only for MgO and CaO. The peak energies of these bands as well as those for the  $F^+$  center bands are summarized in Table 1. The absorption band of the F center arises from an allowed transition from the  $^1A_{1g}$  ground state to one or more  $^1T_{1u}$  excited states. Since the ground state of the F center is diamagnetic, it has no EPR signal and consequently must be detected optically. Both the  $F^+$  and the F

centers in MgO have absorption bands at about 5 eV and this led to some initial uncertainty about the correctness of their identification.<sup>9</sup>

As was noted in the previous section, there have been relatively few theoretical calculations made on the F center in the alkaline earth oxides. Neelcy and Kemp have reported the results of an LCAO (linear combination of atomic orbitals) calculation using Gaussian-type orbitals on the F center in MgO and CaO.<sup>10</sup> This calculation was made using the point-ion lattice model, without taking into account lattice relaxation and polarization corrections. Their prediction for the  $^1A_{1g} \rightarrow ^1T_{1u}$  absorption energy was 5.4 eV in MgO and 4.4 eV in CaO. Bennett has reported a more extensive calculation of the F center in MgO and CaO.<sup>11</sup> His model involved the numerical solution of the Hartree-Fock-Slater equations<sup>12</sup> to obtain the orbitals for the defect electrons centered on an anion vacancy, again using a point-ion lattice potential. The effects of ionic polarization of the nearest neighbor ions and estimates for the correlation energy of the defect electrons were included. Bennett found the absorption energies to be 3.9 eV in MgO and 3.15 eV in CaO. These calculations also predicted energies for the  $^3T_{1u} \rightarrow ^1A_{1g}$  emission peak of 2.53 eV in MgO and 1.93 eV in CaO, and 3.10 eV for the  $^1T_{1u} \rightarrow ^1A_{1g}$  emission peak in CaO. A recent calculation on the F center in MgO and CaO was made by Ermoshkin et al.<sup>13</sup> using a 26-atom cluster in the so-called extended Huckel approximation. They calculated  $^1A_{1g} \rightarrow ^1T_{1u}$  transition energies of 5.4 eV for MgO and 4.17 eV for CaO. Their calculation, which did not allow for lattice distortion or polarization, placed the excited state well above the bottom of the conduction band. Photoconductivity measurements in MgO show the relaxed excited state of the F center to be  $\sim 0.06$  eV below the bottom of the conduction band.<sup>14</sup>

### III. OUTLINE OF THE MODEL

In the model used in making these calculations, the crystal is divided into two regions. Near the defect the electronic structure on the neighboring ions is treated in detail in a Hartree-Fock type approximation, while in the outer region a simple effective mass approximation is used. For the F center, the effective two-electron Hamiltonian including the effects of dielectric polarization but neglecting lattice relaxation is expressable in the form

$$H(1,2) = \sum_{i=1}^2 h(\underline{r}_i) + U_{12}, \quad (1)$$

where the effective one-electron Hamiltonian  $h(\underline{r})$  is described in some detail in Ref. 3. The two-electron interactions, including additional polarization contributions not found in one-electron centers, are contained in  $U_{12}$ .

We approximate the two-electron wave function for this system by the expansion

$$\psi^{\pm}(1,2) = \sum_{k=1}^n c_k \psi_k^{\pm}(\underline{r}_1, \underline{r}_2) \chi_{\pm}(\zeta_1, \zeta_2), \quad (2)$$

in which + implies a singlet state of the F center and - implies a triplet. The spin function  $\chi_{\pm}(\zeta_1, \zeta_2)$  has the usual form, and the two-electron basis function  $\psi_k^{\pm}$  is expressed in terms of one-electron orbitals:

$$\psi_k^{\pm}(\underline{r}_1, \underline{r}_2) = N_k [g_{k1}(\underline{r}_1)g_{k2}(\underline{r}_2) \pm g_{k2}(\underline{r}_1)g_{k1}(\underline{r}_2)], \quad (3)$$

where  $N_k$  is a normalization factor. This notation emphasizes the need to specify two orbitals, i.e.,  $k_1$  and  $k_2$ , in order to determine the  $k$ -th two-electron function. In helium-like atoms, a few terms of the form of Eq. 3 can introduce approximately 85% of the total correlation energy. In the present calculations the one-electron orbitals  $g_{ki}$  are of the form

$$g_{ki}(\underline{r}) = \bar{N}_{ki} [f_{ki}(\underline{r}) - \sum_{vj} \phi_{vj}(\underline{r}) \langle \phi_{vj} | f_{ki} \rangle] , \quad (4)$$

where  $\bar{N}_{ki}$  is an orbital renormalization factor. The index  $v$  runs over all the ions in the inner region and  $\phi_{vj}(\underline{r})$  denotes the  $j$ -th one-electron orbital on the  $v$ -th ion. The functions  $f_{ki}$  are of the form

$$f_{ki}(\underline{r}) = [(2\beta)^{2n+1} / (2n)!]^{1/2} r^{n-1} e^{-\beta r} K_{Tp}(\theta, \phi) . \quad (5)$$

$K_{Tp}$  is the cubic harmonic associated with the  $p$ -th component of the  $\Gamma$ -th irreducible representation of the  $O_h$  point group.

In the present calculations, we typically used six configurations of the type given by Eq. 3 for each state of the F center. The non-linear parameters appearing in Eq. 5 were optimized for each symmetrized displacement of the first-nearest-neighbor ( $1nn$ ) ions. To obtain configuration coordinate curves, the lattice relaxation energy was calculated within the framework of classical ionic theory and added to the electronic energy for the various values of the configuration coordinate.

#### IV. DISCUSSION OF RESULTS

##### A. Calcium Oxide

In our work thus far we have placed the greatest emphasis on the F center in CaO because it has been more thoroughly studied in that crystal than in any of the other alkaline-earth oxides. Our results for the F center in CaO are reported in part in Ref. 15. There we show the absorption and emission configuration coordinate curves for the four lowest electronic levels of the F center. The energy of the  $^1A_{1g} \rightarrow ^1T_{1u}$  transition was set near the experimental value of 3.1 eV by adjusting certain parameters in the model, which then remain fixed during the emission. An analysis of the wave functions associated with the four lowest absorption states shows that both electrons in the  $^1A_{1g}$  ground state are well localized within the vacancy region. On the otherhand, in the  $^3A_{1g}$  and  $^1T_{1u}$  states, the excited electron is almost completely outside the vacancy, and in the  $^3T_{1u}$  state, the charge within the vacancy is a rapidly varying function of the  $A_{1g}$  relaxation of the  $^{40}Ca$  ions. This behavior is illustrated in Table 2 where we give the integrated F center charge within the second-nearest-neighbor distance for each of the four states. We display our results for the emission states of the F center in CaO in Fig. 1, where we plot the energies as a function of the  $A_{1g}$  relaxation of the  $^{40}Ca$  ions. These results differ slightly from those of Ref. 15 due to refinements in our wave functions and minor changes in the model. Both sets of calculations clearly predict that the  $^3T_{1u} \rightarrow ^1A_{1g}$  and the  $^1T_{1u} \rightarrow ^1A_{1g}$  transition should occur at roughly 2.0 eV. These results have been verified by recent studies of the luminescence spectrum by Bates and Wood<sup>16,17</sup>

that was stimulated by our earlier calculations. The F center emission band at low temperatures peaks at 2.01 eV and shows a continuous shift of intensity into a high-energy shoulder at 2.05 eV as the temperature is raised above 300°K. At the same time, the lifetime of the luminescence decreases rapidly indicating that this shoulder is probably associated with the  $^1T_{1u} + ^1A_{1g}$  emission.

Studies of the paramagnetic resonance of the emitting level involved in this emission line at low temperatures clearly showed that it has a substantial spin-triplet component.<sup>18</sup> These measurements further indicated a strong Jahn-Teller coupling to the  $E_g$  vibrational modes and from later work on the stress splittings of the zero-phonon line, it was concluded that the coupling to  $A_{1g}$  and  $T_{2g}$  modes is weak.<sup>19</sup> Our calculation of the coupling of the emission states to the  $A_{1g}$ ,  $E_g$  and  $T_{2g}$  distortions of the first-nearest-neighbor ions indicate that the  $^3T_{1u}$  state is strongly coupled to the  $E_g$  mode. The  $^1T_{1u}$  state is very weakly coupled to the  $E_g$  and  $T_{2g}$  modes due to the diffuseness of the  $t_{1u}$  electron and is dominantly coupled to the  $A_{1g}$  mode. For this state we calculate an  $A_{1g}$  Huang-Rhys factor of 10 and an effective frequency of  $390 \text{ cm}^{-1}$ . Our results for the  $^3T_{1u}$  state are summarized in Table 3. Calculations for  $E_g$  and  $T_{2g}$  distortions were carried out at the minimum value of the  $A_{1g}$  displacements. We assumed that the  $A_{1g}$ ,  $E_g$  and  $T_{2g}$  components of the lattice relaxation simply superimpose, as in linear coupling theory, although the calculations indicated considerable quadratic coupling in the  $^3T_{1u}$  state for  $A_{1g}$  relaxation.

To further support the above interpretation of the 2.0 eV emission band, a calculation was made of the temperature dependence of the band

shapes at temperatures above 25°C.<sup>17</sup> These calculations were based on a model in which two distinct sets of configuration coordinate curves were assumed for the  $^3T_{1u} + ^1A_{1g}$  and  $^1T_{1u} \rightarrow ^1A_{1g}$  luminescence bands. The justification for this assumption is that in the fairly compact  $^3T_{1u}$  electronic state, the coupling to the lattice is primarily by way of the  $E_g$  vibrational modes whereas, in the much more diffuse  $^1T_{1u}$  state, the coupling is principally to  $A_{1g}$  modes. The two sets of curves are interconnected because transitions from the  $^3T_{1u}$  state to the  $^1T_{1u}$  state can occur as the temperature is raised. The results of this calculation are shown in Fig. 2 and are in good agreement with the observed spectra.<sup>17</sup> The emission curves shown in Fig. 1 also suggest the possibility of observing the  $^3T_{1u} \rightarrow ^3A_{1g}$  transition using excited-state absorption spectroscopy. Measurements of this type have been made for the  $X_2^-$  or  $V_k$  center in several alkali halides.<sup>20</sup> Our calculations predict a transition energy of approximately .7 eV.

### B. Magnesium Oxide

The results of our calculations to date on the F center in MgO have been less satisfactory than in CaO due, we believe, to the greater differences in the relative sizes and polarizabilities of the  $Mg^{2+}$  and  $O^{2-}$  ions compared to those of the  $Ca^{2+}$  and  $O^{2-}$  ions in CaO. These differences lead to much larger polarization effects in the emission states and these appear to be primarily responsible for the significantly larger Stokes shift observed in MgO as compared to that in CaO (2.6 eV vs. 1.1 eV). Thus the difficulties alluded to earlier in adequately treating the polarizability of the  $O^{2-}$  ion magnify any inadequacies that are inherent in that part of the model used to treat these effects. For this reason, we

have found it necessary, in the calculation to date, to adjust certain of the emission parameters in our model from their preset values in order to obtain reasonable agreement with the experimental Stokes shift; this adjustment was not necessary in CaO.

Our results for the absorption and emission states of the F center in MgO are given in Figs. 3 and 4 respectively. These figures, as well as those of Ref. 15, show the bottom of the conduction band and a few words concerning its calculation are in order. Within the context of our model, the bottom of the conduction band includes polarization-correlation effects introduced by polaron theory and the energy  $\epsilon(a_{1g})$  of the electron which remains well localized within the vacancy when the excited electron is removed to the bottom of the conduction band. Thus the electronic energy is given by the expression

$$E_{\text{cond}} = \epsilon(a_{1g}) + \epsilon_{\text{HF}} + U_p . \quad (6)$$

The polarization-correlation energy,  $U_p$ , is calculated using the Toyozawa,<sup>21</sup> Haken-Schottky<sup>22</sup> form for the polarization potential. The bottom of the conduction band in these figures depends on the value of the configuration coordinate because it also includes the lattice relaxation energy.

The difference between the configuration coordinate curves for absorption and emission can be explained briefly as follows. In the  $^1A_{1g}$  ground state of the center, the charge density of the two electrons is almost entirely confined to the vacancy, but in the  $^1T_{1u}$  state, even in absorption, the excited electron is almost completely outside of the vacancy. The ions are unable to respond to the change in the effective charge of

the vacancy during the optical transition, but once in the excited state, the ions can adjust to this change and, to some extent, follow the motion of the electron; the diffuse excited states are therefore shifted in energy relative to the compact states.

The integrated F center charge within the second-nearest-neighbor distance for the lowest energy absorption state of each symmetry is given in Table 2. In Fig. 3 we show two excited states of  $^1T_{1u}$  symmetry. The energy separation between these states is 0.2 eV and transitions to both states are probably involved in the F band. We obtain similar results for the F center absorption band in CaO.

A luminescence band associated with the F center absorption in MgO has been observed at roughly 2.4 eV.<sup>9</sup> From the emission curves shown in Fig. 4, we attribute this band to the  $^3T_{1u} \rightarrow ^1A_{1g}$  and  $^1T_{1u} \rightarrow ^1A_{1g}$  transitions. In all of our emission state calculations for this center we find these transitions to be within 0.1 eV of each other. As was true in the case of CaO, the excited electron in the  $^1T_{1u}$  state is very diffuse and the dominant coupling is to the  $A_{1g}$  mode with only weak coupling to the  $E_g$  and  $T_{2g}$  modes. The  $^1T_{1u} \rightarrow ^1A_{1g}$  transition energy is calculated to be 2.5 eV. For this state we calculate an  $A_{1g}$  Huang-Rhys factor of 14 and an effective frequency of  $629 \text{ cm}^{-1}$ . The relaxed excited  $^1T_{1u}$  state shown in Fig. 4 lies 0.03 eV below the bottom of the conduction band. This separation gives good agreement with the 0.06 eV separation predicted by photoconductivity measurements.<sup>14</sup> Our calculations for the coupling of the  $^3T_{1u}$  emission state to the  $A_{1g}$ ,  $E_g$  and  $T_{2g}$  modes are summarized in Table 3. These results predict a much stronger coupling of this state to the  $T_{2g}$  than to the  $E_g$  mode. We calculate a  $^3T_{1u} \rightarrow ^1A_{1g}$  transition energy of 2.55 eV.

Further theoretical analysis of the luminescence of the F center in MgO would be greatly aided by more complete experimental information about the temperature dependence of the bands and about the ordering of the emitting levels. Definitive experiments on the optical paramagnetic resonance properties of MgO comparable in detail to those now available for CaO<sup>18,19</sup> would be very useful.

### C. Strontium Oxide

Little is known experimentally about the F center in SrO, and no prior theoretical studies have been reported. The absorption band for the F center has been identified and peaks at about 2.5 eV;<sup>23</sup> no luminescence bands have been reported.

The results of our calculations for the lowest lying states of the F center in SrO are shown in Fig. 5; they are qualitatively similar to those for the F center in MgO and CaO, but differ markedly in their details. The  $^1A_{1g} \rightarrow ^1T_{1u}$  absorption occurs at 2.47 eV for a 3% outward distortion of the first-nearest-neighbor Sr<sup>2+</sup> ions. We calculate an oscillator strength for this transition of 1.68. For small distortions, the  $^1T_{1u}$  and  $^3A_{1g}$  states were found to be considerably more localized than they were in either MgO or CaO. The integrated charge densities out to second-nearest-neighbors, shown in Table 2, clearly demonstrate the sensitivity of the electronic wave functions for these states to the positions of the nearest neighbor Sr<sup>2+</sup> ions. The rapid variation in the localization of the wave function in the region  $\delta = 0\%$  to  $\delta = 6\%$  accounts for the non-parabolic shape of the energy curves for these states.

Our calculations of the coupling of the  $^1T_{1u}$  state to the  $A_{1g}$ ,  $E_g$  and  $T_{2g}$  modes are summarized in Table 4. These results indicate that the

$^1T_{1u}$  absorption state in SrO is dominantly coupled to the  $T_{2g}$  mode and has relatively weaker coupling to the  $A_{1g}$  and  $E_g$  modes. This is in sharp contrast with the predominant  $A_{1g}$  coupling of the  $^1T_{1u}$  state in MgO and CaO.

The calculated curves predict a  $^1T_{1u} \rightarrow ^1A_{1g}$  emission band at about 1.5 eV. From Table 2 we observe that the excited electron in the  $^1T_{1u}$  state is quite diffuse in the region of the minimum; this is reflected in the dominance of the  $A_{1g}$  coupling of this state in emission. Our calculations for the  $^3T_{1u}$  state reveal a minimum in the  $A_{1g}$  configuration coordinate curve at about a 1% inward distortion of the nearest neighbors relative to the location of the minimum in the ground state curve. Our calculation of the coupling parameters of this state to the  $A_{1g}$ ,  $E_g$  and  $T_{2g}$  modes is summarized in Table 3. They show that the  $^3T_{1u}$  state is dominantly coupled to the  $T_{2g}$  mode and that the Jahn-Teller lowering of the energy is 0.18 eV. We calculate a  $^3T_{1u} \rightarrow ^1A_{1g}$  transition energy of 0.4 eV. This small value may in part account for the fact that a luminescence band has not yet been observed for the F center in SrO.

Our calculations also suggest the possibility of observing the excited state absorption for the  $^3T_{1u} \rightarrow ^3A_{1g}$  transition at about 1.9 to 2.0 eV. Both the  $^3T_{1u}$  and  $^3A_{1g}$  wave functions are compact in the region of the predicted absorption and we calculate an oscillator strength for this transition of 0.4.

## V. SUMMARY

Our calculated results for the F center absorption and emission bands in MgO, CaO and SrO agree reasonably well with available experimental data. This is to be expected for the peak energy of the absorption bands since the calculated and measured positions were forced to coincide approximately by our choice of  $\epsilon_{HF}$  in Eq. 6. Of greater significance is our calculation of the emission states for these centers.

As was mentioned in Section IV, the theoretical emission states shown in Fig. 1 have already proven useful in illuminating several aspects of the emission spectra in CaO. Prior to this study, it was believed that the  $^1T_{1u} \rightarrow ^1A_{1g}$  emission occurred at 2.5 eV, with the  $^3T_{1u} \rightarrow ^1A_{1g}$  occurring at 2.0 eV.<sup>24</sup> A subsequent theoretical calculation<sup>11</sup> lent support to this interpretation of the observed emission spectra. However, all attempts to adjust the parameters in our model to yield emission bands at these two energies while at the same time keeping the absorption at about 3.1 eV failed. In all these calculations, our model consistently predicted that both transitions should occur within about a tenth of an eV of one another. This led to the recent reexamination of the emission spectra of the F center in CaO by Bates and Wood,<sup>16</sup> where they showed that the 2.5 eV band is not related to a transition of the F center. The near degeneracy of the  $^3T_{1u} \rightarrow ^1A_{1g}$  and  $^1T_{1u} \rightarrow ^1A_{1g}$  transitions shows up in the temperature dependence of the 2 eV luminescence band,<sup>17</sup> where a two-peaked structure is observed at 300 C. Our calculations show that at low temperatures, the  $^3T_{1u} \rightarrow ^1A_{1g}$  transition is dominant and as the temperature increases, the  $^1T_{1u} \rightarrow ^1A_{1g}$  band contribution also increases. The calculated strength of the coupling of the  $^3T_{1u}$  electronic state to the  $A_{1g}$ ,  $E_g$  and  $T_{2g}$

vibrational modes in CaO tends to support the conclusions drawn by Edel et al. 18,19 from their optically detected paramagnetic resonance measurements that the Jahn-Teller coupling of this state to the  $E_g$  modes is strong and that to the  $A_{1g}$  and  $T_{2g}$  modes is weak. The results of our calculations, the available experimental data on the band shapes, and the shell model fits to neutron inelastic scattering data from the phonons in CaO put us in a position to calculate both the absorption and emission band shapes for this center. However, the overlap of the F and  $F^+$  bands make it difficult to determine the absorption band shape experimentally. Unlike the absorption band the emission band at low temperatures is well defined; it shows a zero-phonon line and considerable vibronic structure. We are in the process of calculating the emission band shape and will report on it at a later time.

Comparisons similar to those made above of our results for the emission states of the F center in MgO are hampered by the absence of experimental studies on the 2.4 eV luminescence band in MgO of the kind described for CaO; a luminescence band associated with the F center in SrO has not been reported. Further studies of the shape of the F center absorption band in SrO, similar to those of Hughes and Webb<sup>25</sup> for the  $F^+$  center in that crystal, are needed. They might establish the existence and the nature of the Jahn-Teller coupling in the  $^1T_{1u}$  state which the calculations tentatively predict.

Our results for the F center in all three crystals suggest that excited state spectroscopy within the triplet sub-system of levels should be possible. The long lifetime of the  $^3T_{1u}$  state should make a pseudo two-photon type of experiment feasible. As well as being of intrinsic

interest, the results would provide useful information about the predictions of our calculations and, more importantly, about the nature of the Jahn-Teller couplings in the  $^3T_{1u}$  state.

#### ACKNOWLEDGMENTS

We would like to thank J. B. Bates for his measurements of the emission bands in CaO and his general interest in the problem. We would also like to thank Mark Mostoller for help with certain aspects of the calculations, and Frank A. Modine, M. M. Abraham and Y. Chen for several useful discussions.

REFERENCES

1. HUGHES A. E. and HENDERSON B., in *Point Defects in Crystals*, ed. by J. H. Crawford, Jr. and L. M. Slifken (Plenum Press, New York, 1972).
2. WOOD R. F. and JOY H. W., Phys. Rev. 136 (1964) A451.
3. ÖPIK U. and WOOD R. F., Phys. Rev. 179 (1969) 772.
4. WOOD R. F. and ÖPIK U., Phys. Rev. 179 (1969) 783.
5. WOOD R. F. and ÖPIK U., Phys. Rev. 162 (1967) 736.
6. WOOD R. F. and GILBERT R. L., Phys. Rev. 162 (1967) 746.
7. MEYER A. and WOOD R. F., Phys. Rev. 133 (1964) A1436.
8. WOOD R. F., Phys. Rev. 151 (1966) 692.
9. KAPPERS L. A., KROES R. L. and HENSLEY E. B., Phys. Rev. B 1 (1970) 4151.
10. NEELEY V. I. and KEMP J. C., Bull. Am. Phys. Soc. 8 (1963) 484.
11. BENNETT H. S., Phys. Rev. B 1 (1970) 1702.
12. SLATER J. C., Phys. Rev. 81 (1951) 385.
13. ERMOSHKIN A. N., EVARESTOV R. A. and KOTOMIN E. G., Phys. Stat. Sol. (b) 73 (1976) 81.
14. ROBERTS R. W. and CRAWFORD, JR., J. H., J. Non-Metals 2 (1974) 133.
15. WOOD R. F. and WILSON T. M., Solid State Commun. 16 (1975) 545.
16. BATES J. B. and WOOD R. F., Phys. Letters 49A (1974) 389.
17. BATES J. B. and WOOD R. F., Solid State Commun. 17 (1975) 201.
18. EDEL P., HENNIES C., MERLE D'AUBIGNÉ Y., ROMESTAIN R. and TWARAWSKI Y., Phys. Rev. Letters 28 (1972) 1268.
19. EDEL P., MERLE D'AUBIGNÉ Y. and LOUAT R., J. Phys. Chem. Solids 35 (1974) 67.
20. WILLIAMS R. T. and KABLER M. N., Phys. Rev. B 9 (1974) 1897.

21. TOYOZAWA Y., Prog Theoret. Phys. (Kyoto) 12 (1954) 422.
22. HAKEN H. and SCHOTTKY W., Z. Physik Chem. (Frankfort) 16 (1958) 218.
23. JOHNSON B. P. and HENSLEY E. B., Phys. Rev. 180 (1969) 931.
24. HENDERSON B., STOKOWSKI S. E. and ENSIGN T. C., Phys. Rev. 183 (1969) 826.
25. HUGHES A. E. and WEBB A. P., Solid State Commun. 13 (1973) 167.

TABLE 1.  $F^+$  AND F CENTER OPTICAL DATA.  
ENERGIES ARE GIVEN IN eV.

|     | Absorption         |                    | Emission   |                     |
|-----|--------------------|--------------------|--|---------------------|
|     | F                  | $F^+$              | F  | $F^+$               |
| MgO | 5.0 <sup>a,b</sup> | 4.95 <sup>c</sup>  | 2.4 <sup>b</sup>   | 3.13 <sup>a,b</sup> |
| CaO | 3.1 <sup>d</sup>   | 3.7 <sup>e,f</sup> | 2.05( $^1T_{1u} \rightarrow ^1A_{1g}$ ) <sup>g</sup><br>2.01( $^3T_{1u} \rightarrow ^1A_{1g}$ ) <sup>h,g</sup> | 3.3 <sup>h</sup>    |
| SrO | 2.5 <sup>i</sup>   | 3.1 <sup>e</sup>   | -----  | 2.42 <sup>j</sup>   |
| BaO | 2.3 <sup>k</sup>   | 2.0 <sup>e</sup>   | -----  | -----               |

<sup>a</sup>CHEN Y., KOLOPUS J. L. and SIBLEY W. A., Phys. Rev. 186 (1969) 869.

<sup>b</sup>Reference 9.

<sup>c</sup>HENDERSON B. and KING R. D., Phil. Mag. 13 (1966) 1149.

<sup>d</sup>WARD W. C. and HENSLEY E. B., Phys. Rev. 175 (1968) 1230.

<sup>e</sup>BESSENT R. G., CAVENETT B. C. and HUNTER I. C., J. Phys. Chem. Solids 29 (1968) 1523.

<sup>f</sup>KEMP J. C., ZINIKER W. M., GLAZE J. A. and CHENG J. C., Phys. Rev. 171 (1968) 1024.

<sup>g</sup>Reference 17.

<sup>h</sup>HENDERSON B., CHEN Y. and SIBLEY W. A., Phys. Rev. B 6 (1972) 4060.

<sup>i</sup>Reference 23.

<sup>j</sup>EVANS B. D. and KEMP J. C., Phys. Rev. B 2 (1970) 4179.

<sup>k</sup>ROSE B. H. and HENSLEY E. B., Phys. Rev. Letters 29 (1972) 861.

TABLE 2

INTEGRATED CHARGE WITHIN THE 2nn SHELL OF IONS AS A  
FUNCTION OF THE  $A_{1g}$  OUTWARD DISTORTION OF THE 1nn IONS  
FOR THE LOWEST ENERGY STATE OF EACH SYMMETRY.

| MgO        |            |            |            |            |
|------------|------------|------------|------------|------------|
| $\delta^a$ | $^1A_{1g}$ | $^3A_{1g}$ | $^1T_{1u}$ | $^3T_{1u}$ |
| 0          | 1.97       | 1.05       | 1.20       | 1.90       |
| 2          | 1.96       | 1.03       | 1.08       | 1.85       |
| 4          | 1.94       | 1.01       | 1.03       | 1.76       |
| 6          | 1.93       | 1.01       | 1.01       | 1.59       |
| 8          | 1.90       | 1.01       | 1.00       | 1.28       |
| 10         | 1.86       | 0.99       | 0.99       | 1.08       |

| CaO        |            |            |            |            |
|------------|------------|------------|------------|------------|
| $\delta^a$ | $^1A_{1g}$ | $^3A_{1g}$ | $^1T_{1u}$ | $^3T_{1u}$ |
| 0          | 1.98       | 1.05       | 1.04       | 1.93       |
| 2          | 1.98       | 1.02       | 1.01       | 1.88       |
| 4          | 1.97       | 1.01       | 1.01       | 1.72       |
| 6          | 1.96       | 1.01       | 1.00       | 1.52       |
| 8          | 1.93       | 1.00       | 1.00       | 1.05       |
| 10         | 1.89       | 1.00       | 1.00       | 1.01       |

| SrO        |            |            |            |            |
|------------|------------|------------|------------|------------|
| $\delta^a$ | $^1A_{1g}$ | $^3A_{1g}$ | $^1T_{1u}$ | $^3T_{1u}$ |
| 0          | 1.90       | 1.81       | 1.82       | 1.90       |
| 2          | 1.87       | 1.65       | 1.59       | 1.87       |
| 4          | 1.82       | 1.21       | 1.18       | 1.81       |
| 6          | 1.75       | 1.11       | 1.02       | 1.69       |
| 8          | 1.73       | 1.03       | 1.01       | 1.57       |
| 10         | 1.64       | 1.00       | 1.00       | 1.03       |

<sup>a</sup> $\delta$  measures the outward distortion of the 1nn ions in  
% of the perfect lattice anion-cation distance.

TABLE 3. SUMMARY OF RESULTS FOR THE COUPLING OF THE  
 $^3T_{1u}$  EMISSION STATE TO THE LATTICE MODES.  
 FREQUENCIES ARE GIVEN IN UNITS OF  $\text{cm}^{-1}$  AND  
 ENERGIES ARE IN eV.

|                  | MgO                      | CaO                      | SrO                      |
|------------------|--------------------------|--------------------------|--------------------------|
| $S_{A_{1g}}$     | 1.4                      | 0.1                      | 1.1                      |
| $S_{E_g}$        | 0.3                      | 2.1                      | 0.6                      |
| $S_{T_{2g}}$     | 2.2                      | 0.8                      | 8.5                      |
| $\nu_{A_g}$      | 457                      | 331                      | 175                      |
| $\nu_{E_g}$      | 423                      | 266                      | 149                      |
| $\nu_{T_{2g}}$   | 434                      | 286                      | 169                      |
| $E_{JT}(E_g)$    | -0.02 ( $\delta_Z > 0$ ) | -0.07 ( $\delta_Z > 0$ ) | -0.01 ( $\delta_Z < 0$ ) |
| $E_{JT}(T_{2g})$ | -0.12                    | -0.03                    | -0.18                    |

TABLE 4. SUMMARY OF RESULTS FOR THE COUPLING OF THE  
 $t_{1u}$  ABSORPTION STATE IN SrO TO THE LATTICE.  
FREQUENCIES ARE GIVEN IN UNITS OF  $\text{cm}^{-1}$  AND  
ENERGIES ARE IN eV.

| Mode     | S     | $E_{JT}$ | v     |
|----------|-------|----------|-------|
| $A_{1g}$ | 2.43  | --       | 226.4 |
| $E_g$    | 0.86  | -0.016   | 151.6 |
| $T_{2g}$ | 12.39 | -0.257   | 167.4 |

FIGURE CAPTIONS

Fig. 1. CaO F center emission.  $A_{1g}$  lattice relaxation.

Fig. 2. Calculated luminescence spectra of F centers in CaO.

Fig. 3. MgO F center absorption.  $A_{1g}$  lattice relaxation.

Fig. 4. MgO F center emission.  $A_{1g}$  lattice relaxation.

Fig. 5. SrO F center absorption and emission.  $A_{1g}$  lattice relaxation.

ORNL-DWG 76-5848R

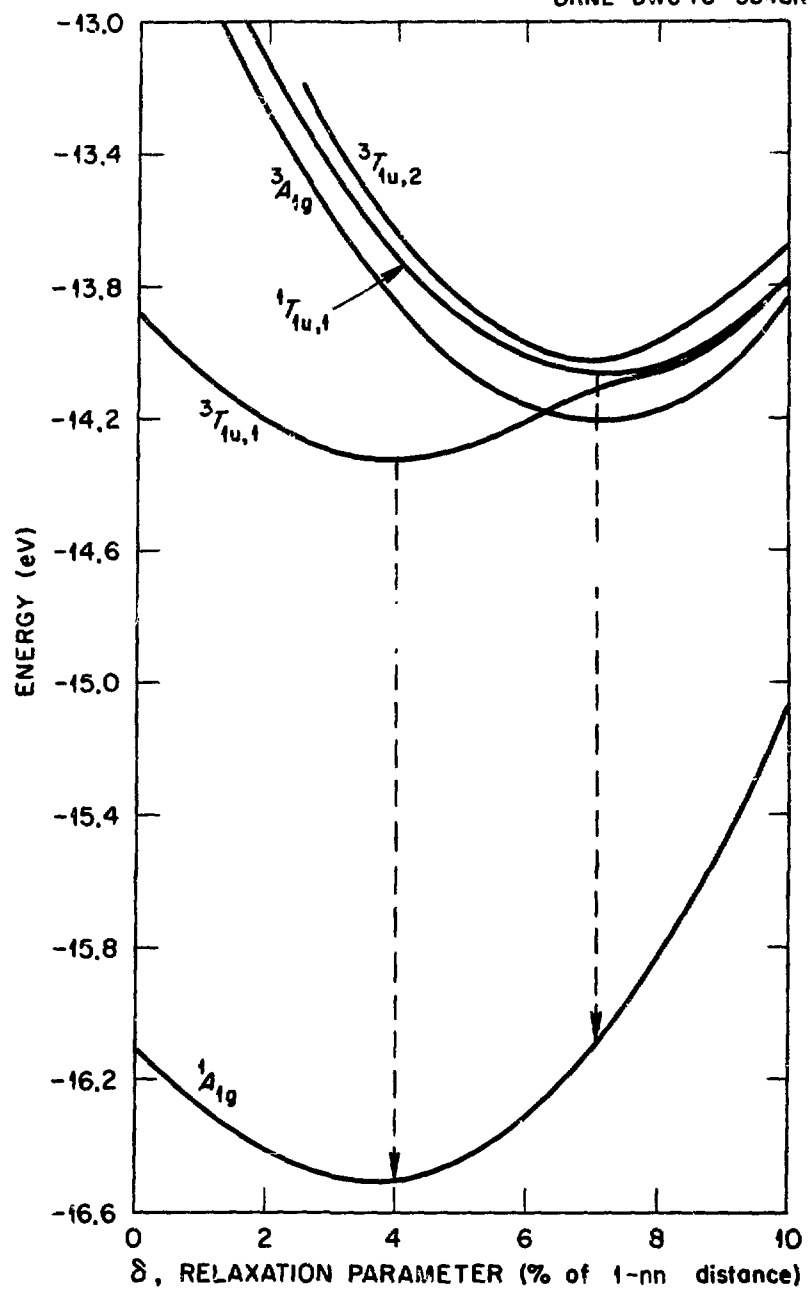


Fig. 1

ORNL-DWG 75-1585

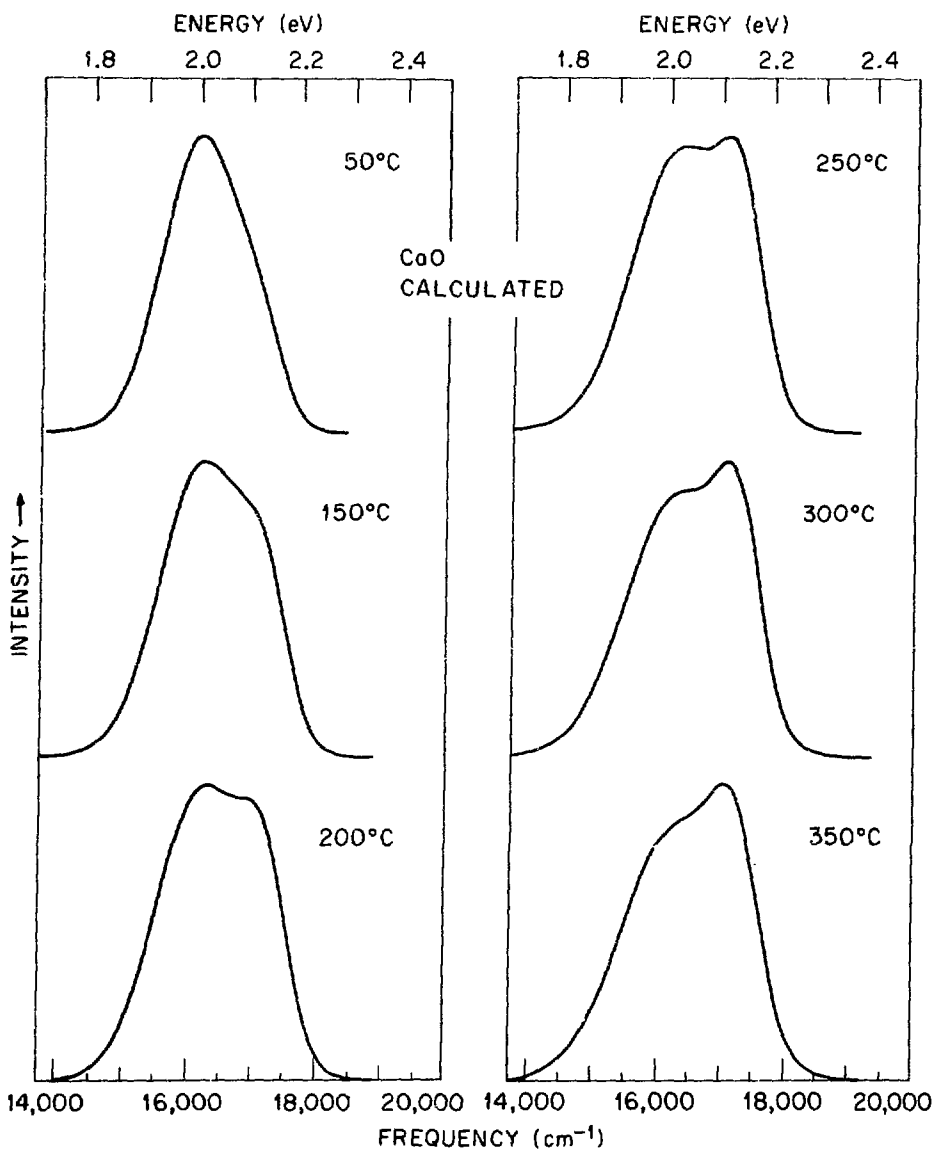


Fig. 2

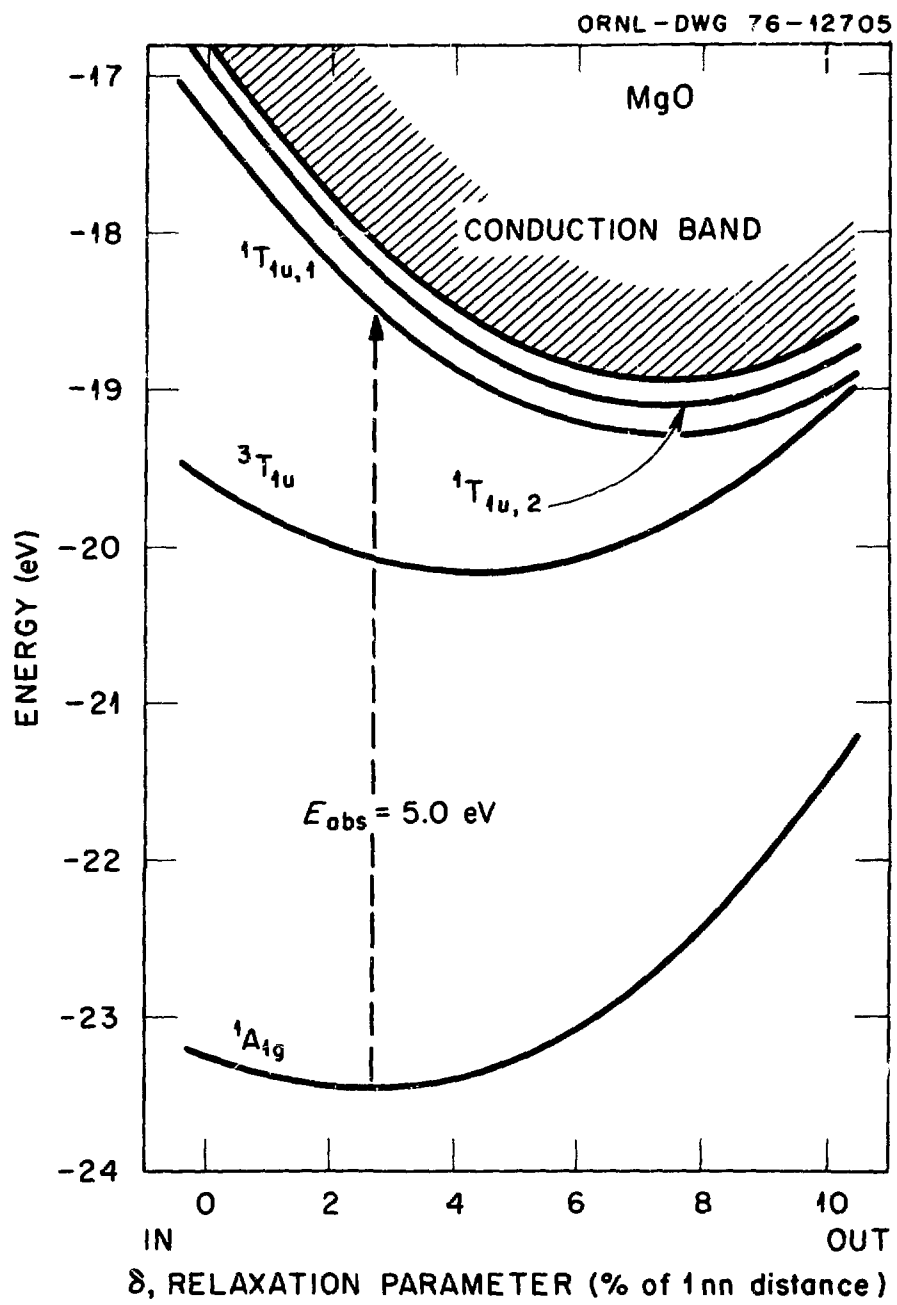


Fig. 3

ORNL-DWG 76-12704

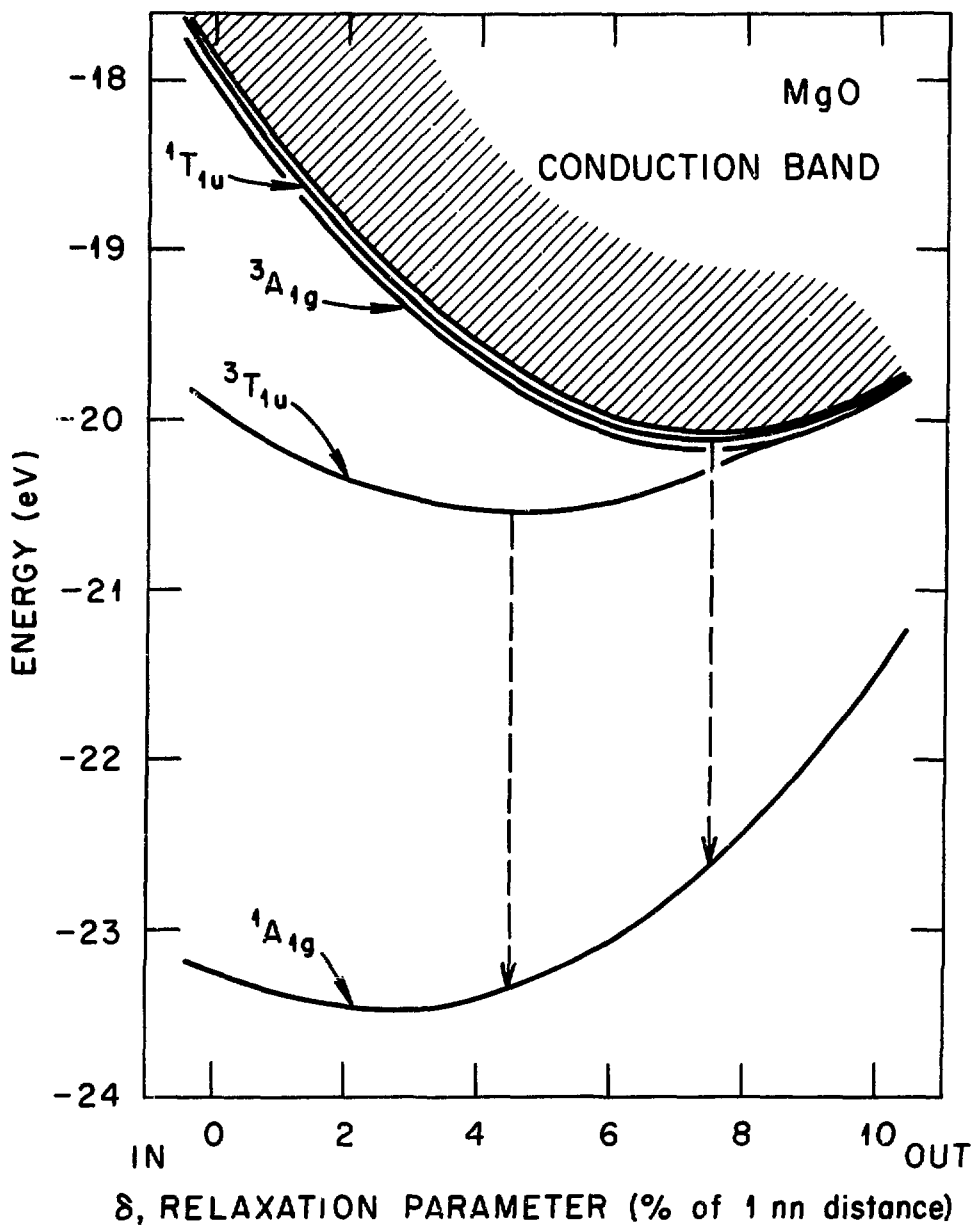


Fig. 4

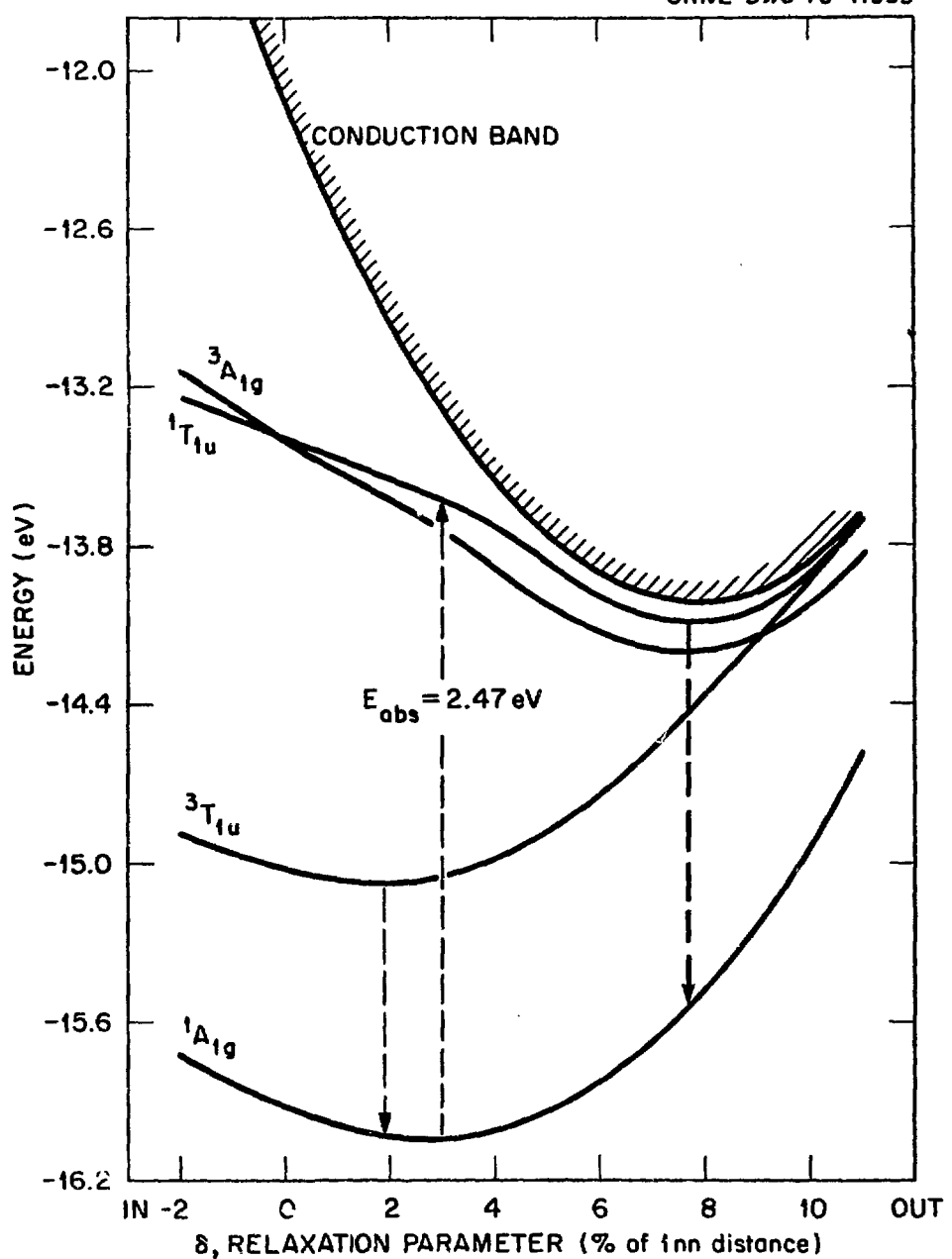


Fig. 5